Electronic Supplementary Material (ESI) for Nanoscale Advances.

Supporting Information

MOF-templated Cobalt Nanoparticles Embedded in Nitrogen-doped Porous Carbon: A Bifunctional Electrocatalyst for Overall Water Splitting

Karabi Nath,[a] Kousik Bhunia,[b] Debabrata Pradhan[b] and Kumar Biradha[a]*

[a] Department of Chemistry, Indian Institute of Technology, Kharagpur-721302, India
Fax: 91-3222-282252; Tel: 91-3222-283346 E-mail: kbiradha@chem.iitkgp.ernet.in

[b] Materials Science Centre, Indian Institute of Technology, Kharagpur-721302, India

---

Contents:

General Aspects:

All chemicals including anthracene, paraformaldehyde, and dimethyl-5-hydroxyisophthalate were obtained from Sigma-Aldrich. All other solvents including glacial acetic acid and HBr were freshly distilled prior to use. Fourier transform IR (FTIR) spectra were recorded with a Perkin-Elmer instrument. Thermogravimetric analysis (TGA) data were recorded under nitrogen atmosphere at a heating rate of 5ºC/min with a Perkin-Elmer instrument, Pyris Diamond TG/DTA. Powder X-ray diffraction (PXRD) data were recorded with a BRUKER-AXS-D8-ADVANCE diffractometer at room temperature ^1H NMR (200/400/600 MHz) spectra were recorded on a BRUKER-AC 200/400/600 MHz. spectrometer. Melting points were recorded using a Fisher Scientific melting point apparatus cat. No. 12-144-1. The surface morphology of the samples were characterized by using a field emission scanning electron microscope (ZEISS EVO 60 with oxford EDS detector). The samples were also characterized through TEM (FEI-TECNAI G^2 20S-TWIN, Type-5022/22) microscopic analysis. An optical image analyzer (Leica DMLM) instrument was used to obtain the optical images of the samples. X-ray photoelectron spectroscopy (XPS) was performed in a ESCALAB Xi, Thermo-Scientific, UK, having a monochromatic Al Kα X-ray source (1486.6 eV). The CAE (constant analyzer energy) for survey spectra is 100 eV and that for high resolution spectra is 50 eV.

Section S1: Synthesis of H_4AOIA and characterization

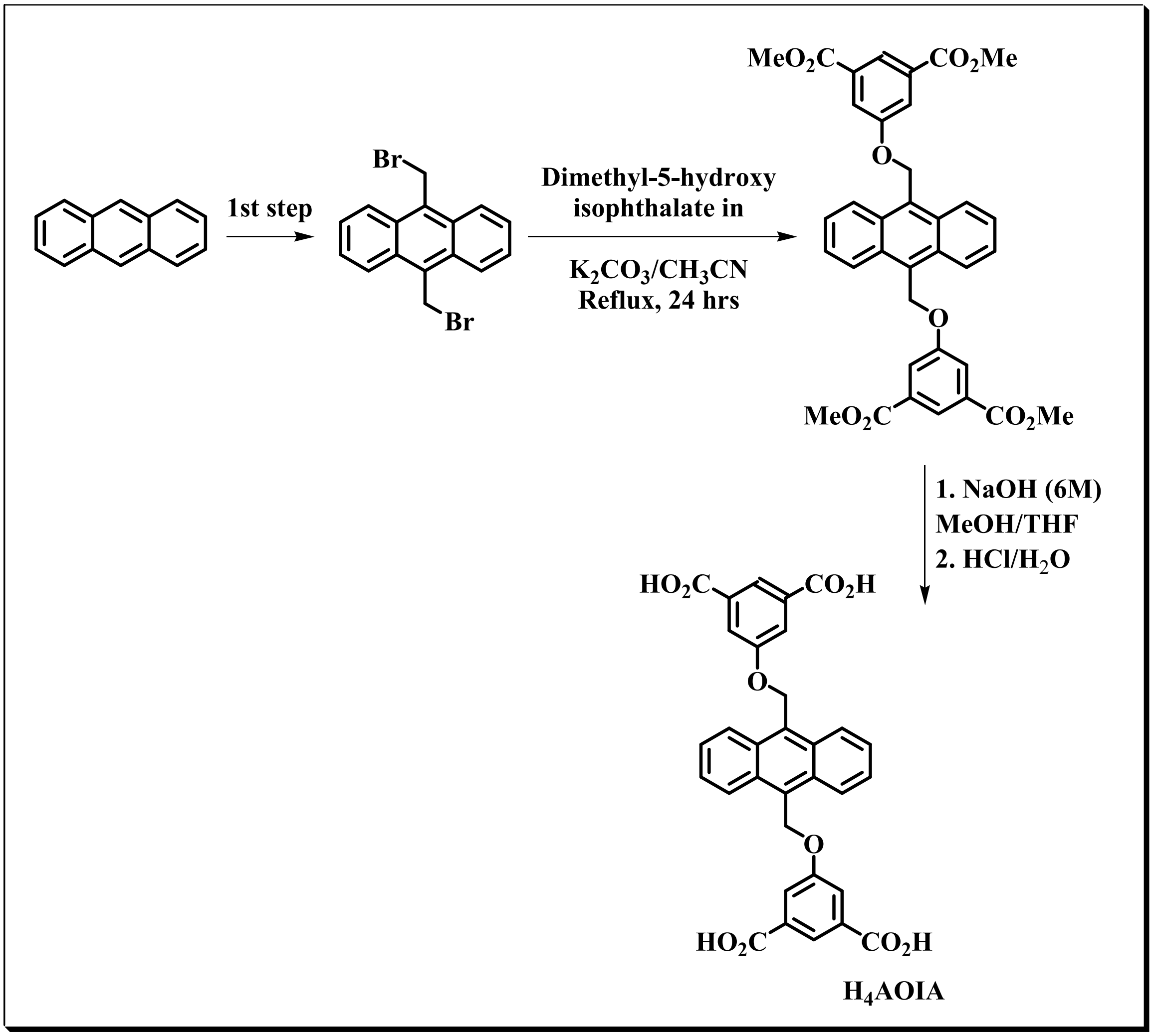

Preparation of the ester: 9,10-Bis-bromomethyl anthracene was prepared in the first step from anthracene following a reported literature procedure.[S1] In the second step, a mixture of dimethyl 5-hydroxy isophthalate (919 mg, 4.38 mmol) and K_2CO_3 (908 mg, 6.57 mmol) was taken in a two neck RB in presence of dry acetonitrile solvent and heated for at least half an hour at 80°C. After this, 9,10-bis-bromomethyl anthracene (800 mg, 2.19 mmol) was added into this reaction mixture and the entire solution was refluxed at 80°C for 24 hrs. The reaction was thereafter quenched by adding water and leading to the formation of a yellow precipitate. The precipitate was filtered and washed thoroughly with water and then dried under vacuum. The resulting tetra methyl ester obtained here was used in the next step for hydrolysis. Yield = 90%,

Hydrolysis of ester: The tetramethyl ester (500 mg, 0.8 mmol) was taken in a RB in presence of MeOH/THF solvent mixture. 6M NaOH solution was added into this and the solution was stirred at room temperature for 48 hrs. After this, the solution was worked up with aqueous HCl, leading to the formation of the tetra-acid (**H_4AOIA**) as a yellow precipitate. The resulting precipitate was washed thoroughly with water for several times and dried under vacuum. The product was further characterized by ^{1}H NMR and ^{13}C NMR spectroscopy.

Yield = 85%, m.p = 240-242 °C.

^{1}H NMR Spectrum of H_4AOIA in d_6-DMSO:-

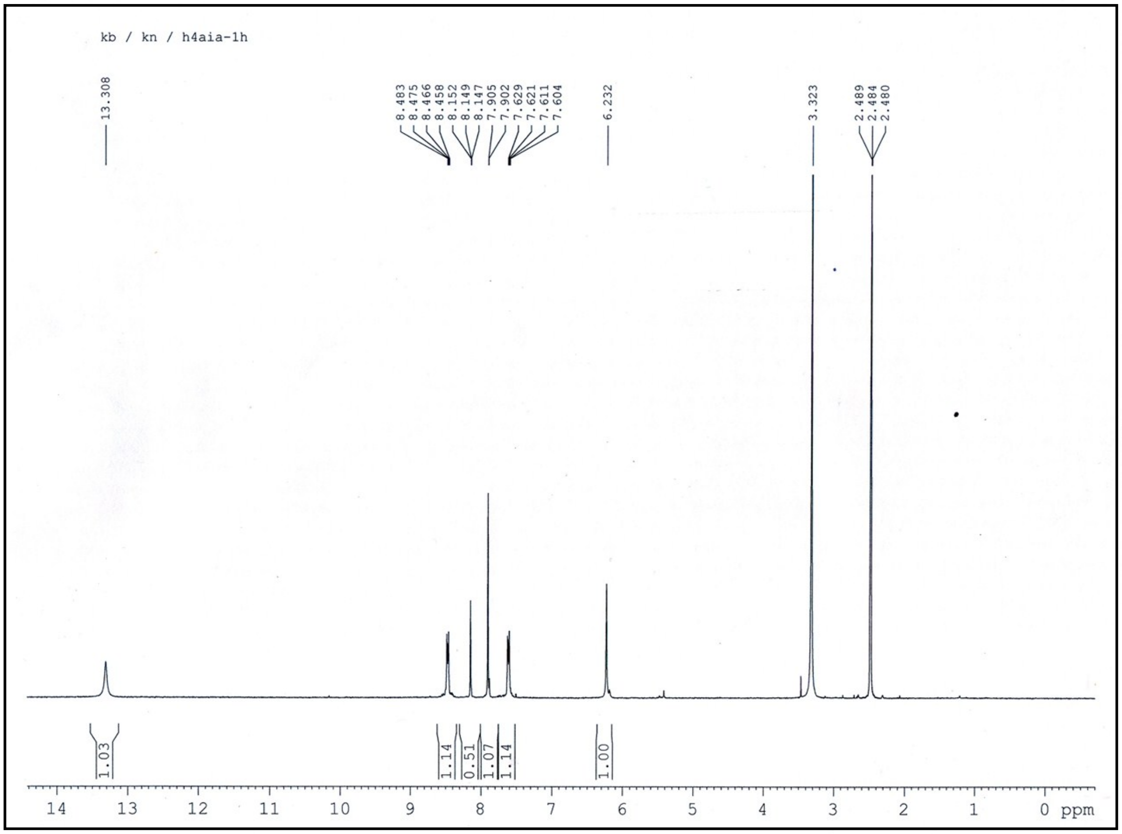

^{13}C-NMR Spectrum of H_4AOIA in d_6-DMSO:-

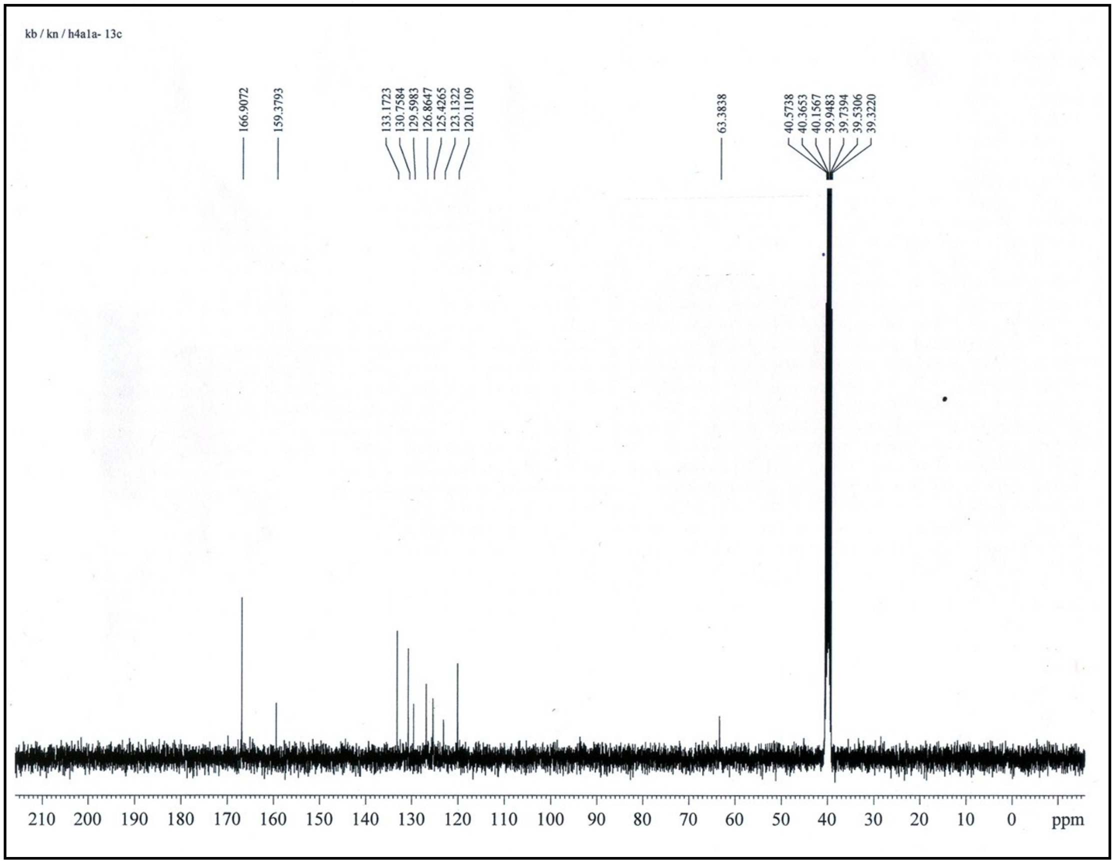

Section S2: Synthesis of Co-AOIA

The as-synthesized ligand **H_4AOIA** (28.3 mg, 0.05 mmol) was mixed with $Co(NO_3)_2$ (29 mg, 0.1 mmol) in presence of DMF (3 ml), H_2O (1 ml) and aqueous HBF_4 (200 µl). The resulting mixture was taken in a 15 ml Pyrex tube and heated in an oven at 80^{o}C for 24 hrs. Dark red crystals of **Co-AOIA** were obtained after cooling down to room temperature. Yield: 70%.

Section S3: Single Crystal Structure Analysis

Crystal Structure Determination:

The single crystal data was collected on a Bruker-APEX-II CCD X-ray diffractometer that uses graphite monochromated Mo Kα radiation ($\lambda = 0.71073$ Å) at low temperature (100 K) by the. hemisphere method. The structure was solved by direct methods and refined by least-squares methods on F^2 using SHELXL-2014.[S2] Non-hydrogen atoms were refined anisotropically, and hydrogen atoms were fixed at calculated positions and refined using a riding model. The H atoms attached to the O atom or N atoms are located wherever possible and refined using the riding model.

Table S1: Crystallographic parameters for Co-AOIA

Formula	$C_{54}H_{41}Co_3N_2O_{27}$
Mol.Wt.	1326.68
T (K)	100(2)
System	Monoclinic
Space group	$P2_1/c$
a (Å)	10.9566(10)
b (Å)	29.918(3)
c (Å)	19.7301(2)
α (°)	90.00
β (°)	99.639(2)
γ (°)	90.00
V (A^3)	6376.2(10)
Z	4
D(g/cm^3)	1.382
R_1 [$I > 2\sigma(I)$]	0.0542
wR_2 (on F^2, all data)	0.1690

Section S4: Powder XRD Patterns

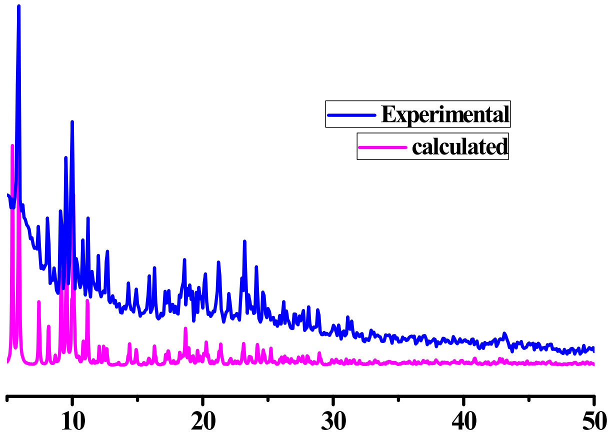

Figure S1. Experimental and calculated powder patterns of **Co-AOIA**

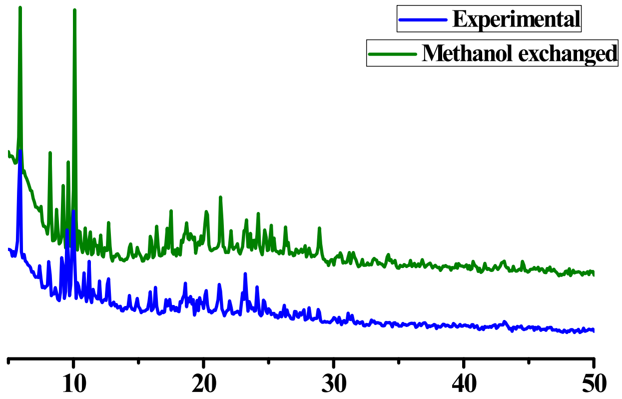

Figure S2. Experimental powder patterns of **Co-AOIA** after solvent exchange in methanol.

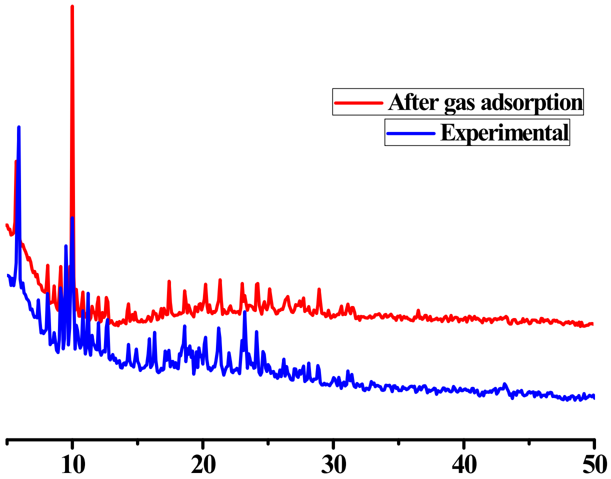

Figure S3. Experimental powder patterns of **Co-AOIA** after gas adsorption analysis.

<u>Section S5</u>: FTIR Spectral Analysis

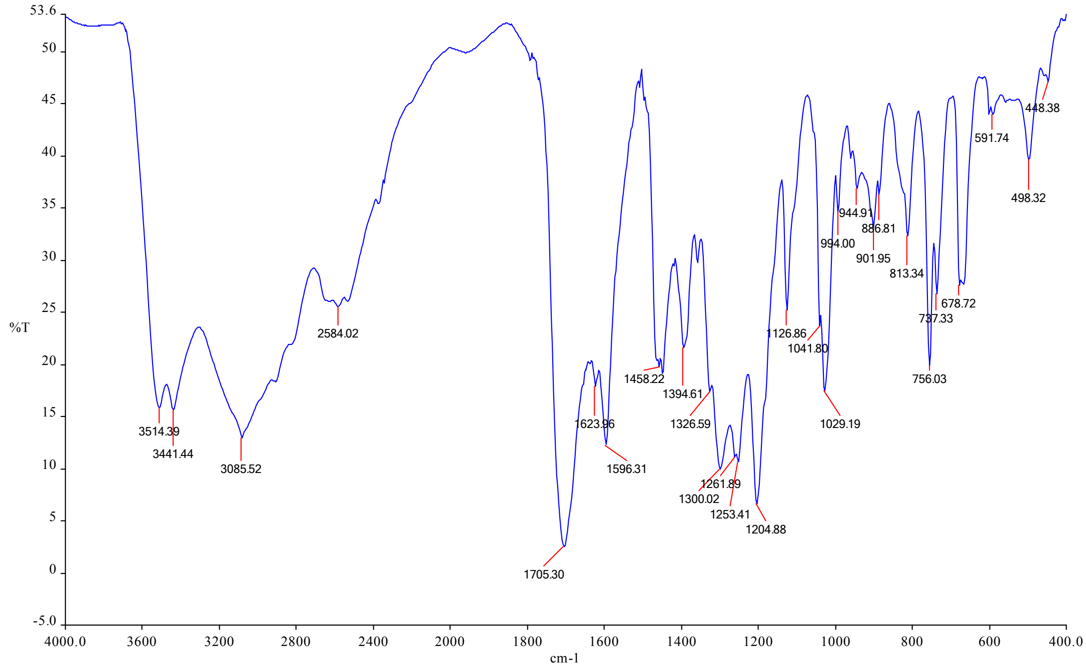

Figure S4. FTIR Spectra of **H_4AOIA**

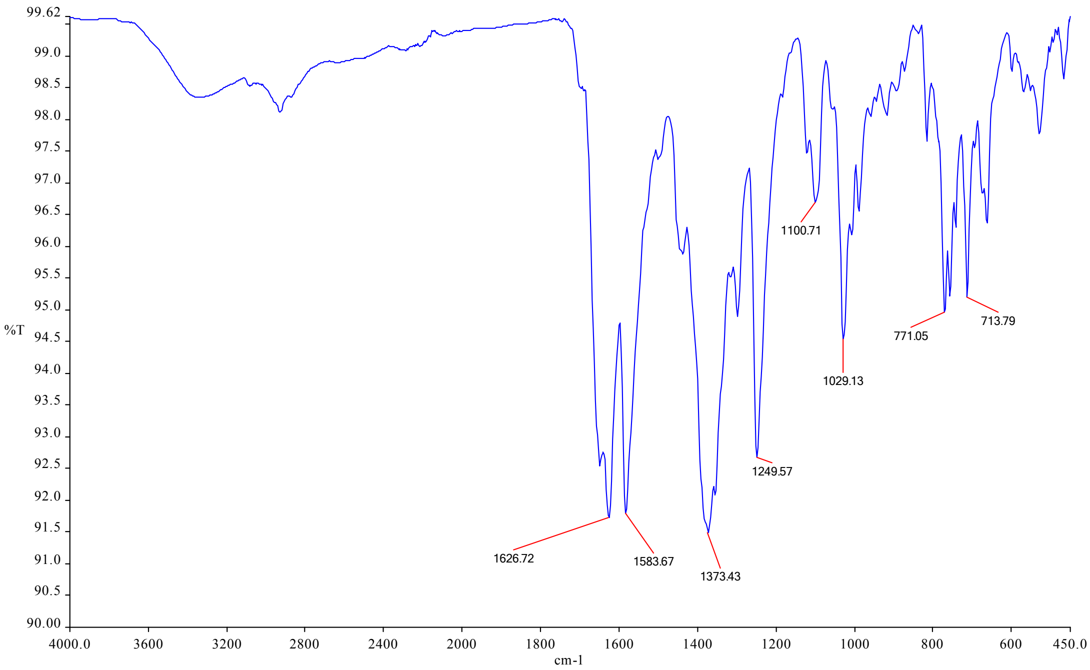

Figure S5. FTIR Spectra of **Co-AOIA**

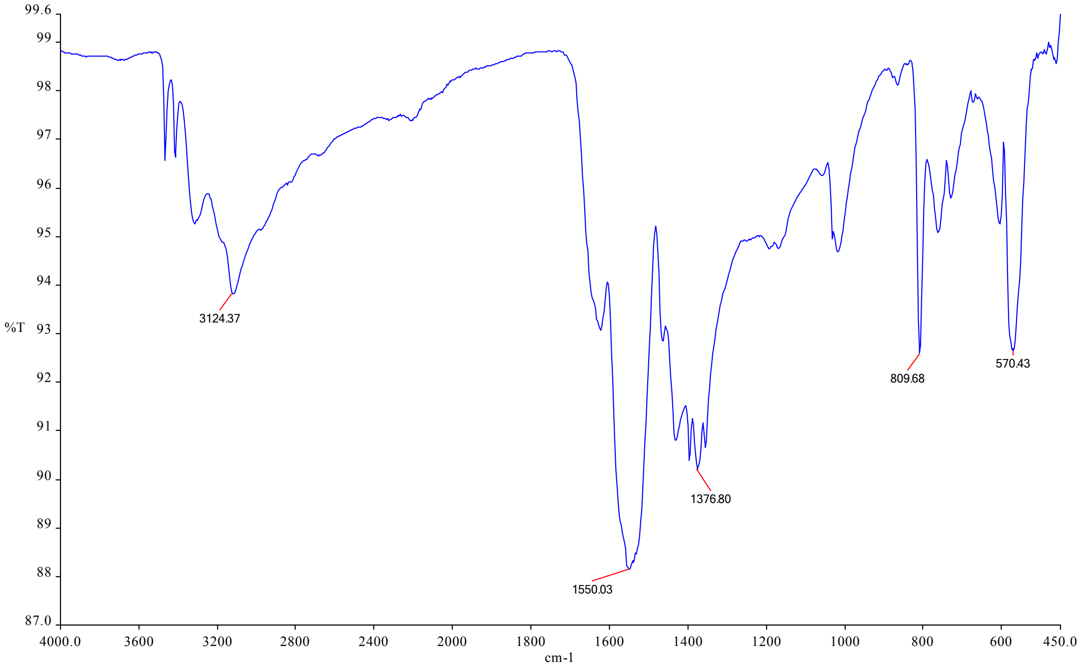

Figure S6. FTIR Spectra of **Co@NPC**

<u>Section S6</u>: Thermogravimetric Analysis (TGA) in Nitrogen-atmosphere

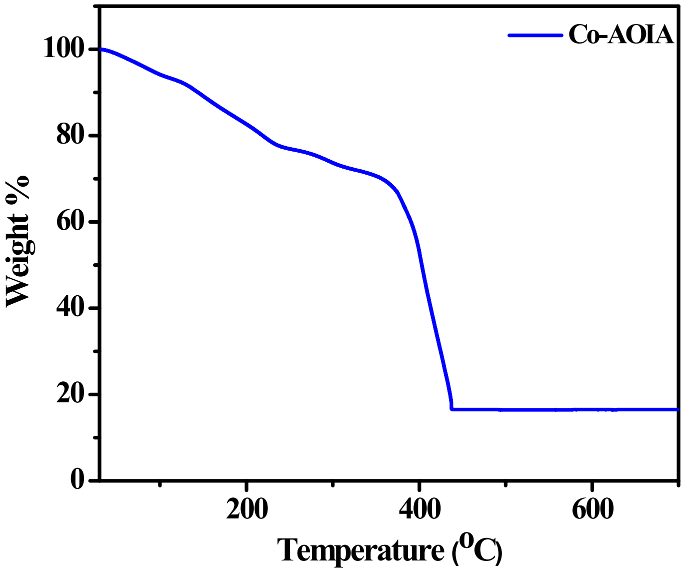

Figure S7. Determination of thermal stability of **Co-AOIA**

Section S7: Synthesis of Co@NPC and bare NPC

Co@NPC: For the preparation of **Co@NPC**, the cobalt MOF (**Co-AOIA**) was carbonized at an optimum temperature of 800°C under an argon atmosphere for 4 hrs. The temperature inside the furnace was gradually raised from room temperature to the target temperature at a heating rate of 10°C/min. The resulting black powder obtained after cooling was then harvested in about 30 % yield.

bare NPC (N-doped porous carbon): The as-synthesized **Co@NPC** was washed extensively with concentrated acids for 24 hrs to remove the Co species, leading to the formation of N-doped porous carbon, represented as bare **NPC**.

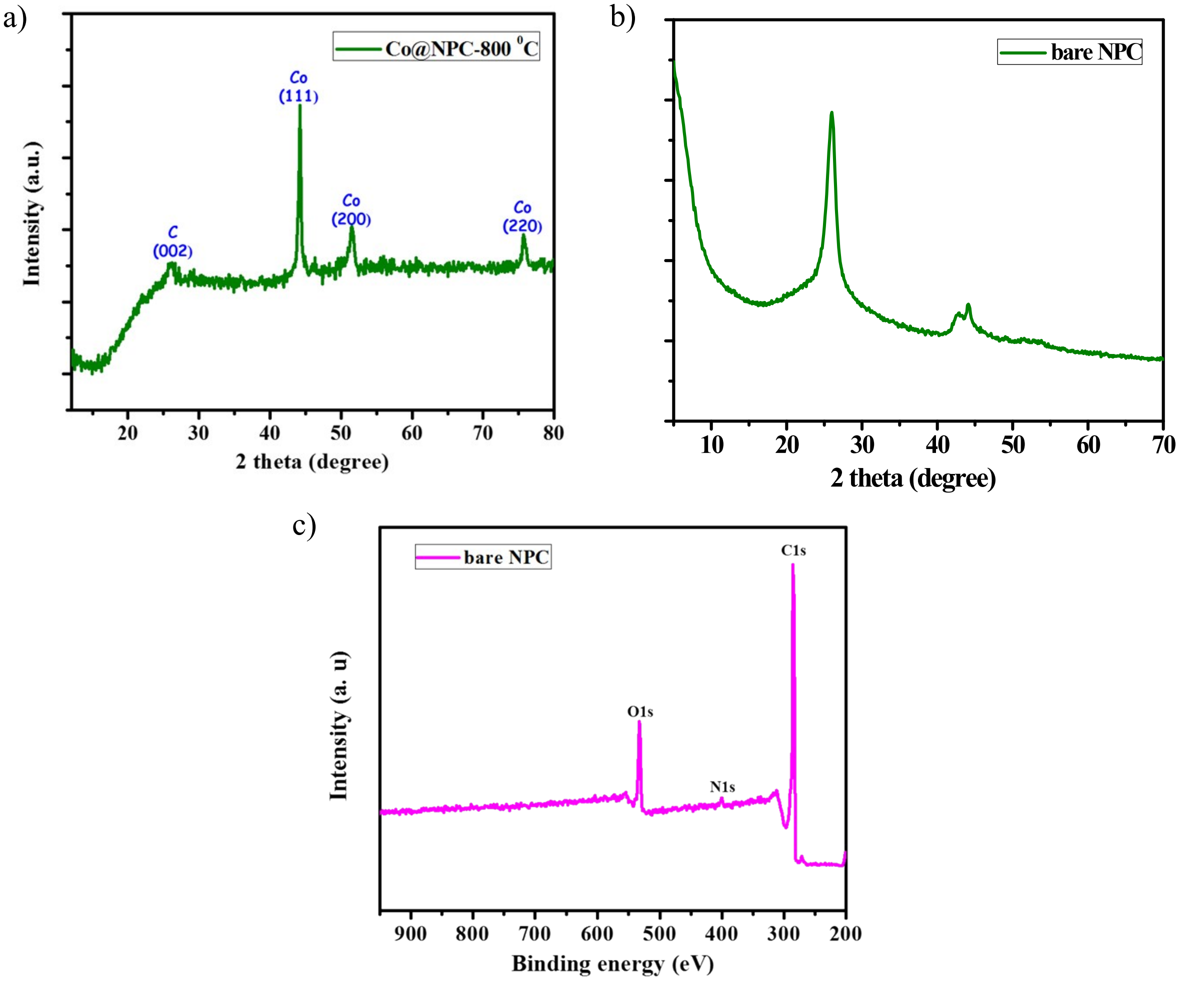

Figure S8. a) Powder pattern of **Co@NPC** formed after carbonization of **Co-AOIA** at 800°C under argon atmosphere; b) powder pattern of bare **NPC** (N-doped porous carbon) obtained after acid wash; c) XPS full survey spectrum of bare **NPC**.

<u>Section S8</u>: Microscopic Analysis, EDS and Mapping

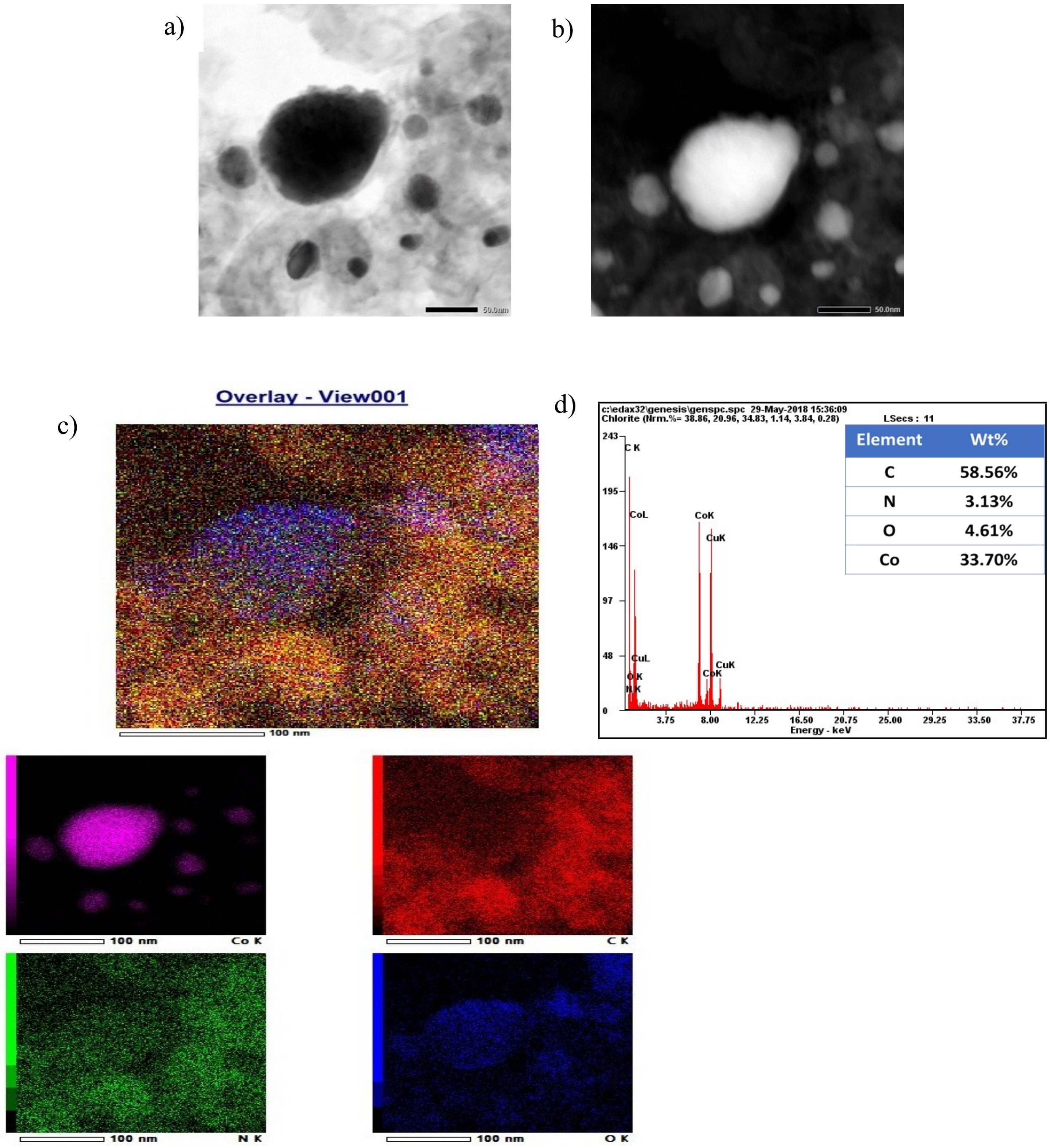

Element	Wt%
C	58.56%
N	3.13%
O	4.61%
Co	33.70%

Figure S9. a) and b) High angle annular dark-field (HAADF) images of **Co@NPC**; c) STEM images and its corresponding elemental mapping; d) EDS spectrum of **Co@NPC**.

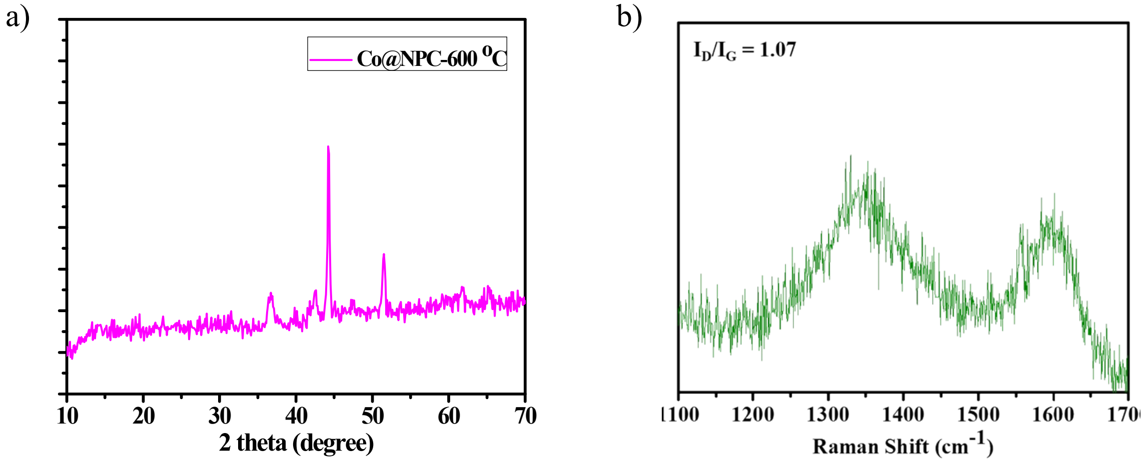

Figure S10. a) Powder pattern showing the presence of both cobalt oxides and metallic cobalt nanoparticles in **Co@NPC-600°C**; b) Raman spectra for **Co@NPC-600°C**.

Section S9: Gas Adsorption Analysis

Nitrogen gas sorption experiment was performed using a Micromeritics 3-Flex Surface Characterization Analyzer (with micropore ports) instrument. Prior to gas adsorption analysis, the as-synthesized **Co-AOIA** crystals were exchanged with methanol solvent for about seven days. The crystals were exchanged with fresh methanol for several times during the time period. The methanol exchanged crystals were then transferred into the sample cell for further activation before the measurement. The activation was performed by using the "outgasser" function of the instrument for a period of 12 hrs at 80°C.

However, **Co@NPC** was activated at 160°C for about 12 hrs prior to measurements of the isotherms. The Brunauer−Emmett−Teller (BET) surface area was then calculated from the N_2 sorption isotherms at 77 K and 1 bar pressure.

The N_2 gas sorption isotherm revealed the typical microporous nature of **Co-AOIA**, as indicated by the reversible type-I behavior, and the BET (Brunauer-Emmett-Teller) surface area was calculated to be 703 m^2/g, at 77K and 1 bar pressure. However, **Co@NPC** exhibited an intermediate pattern of type-I and type-IV isotherms, with sharp uptakes at relatively low pressure and prominent H3-type hysteresis loops within the pressure range from 0.4-1.0, justifying the existence of both microporous and mesoporous structures. The BET surface area of **Co@NPC** was determined to be 179 m^2/g, much lower than that of **Co-AOIA.**

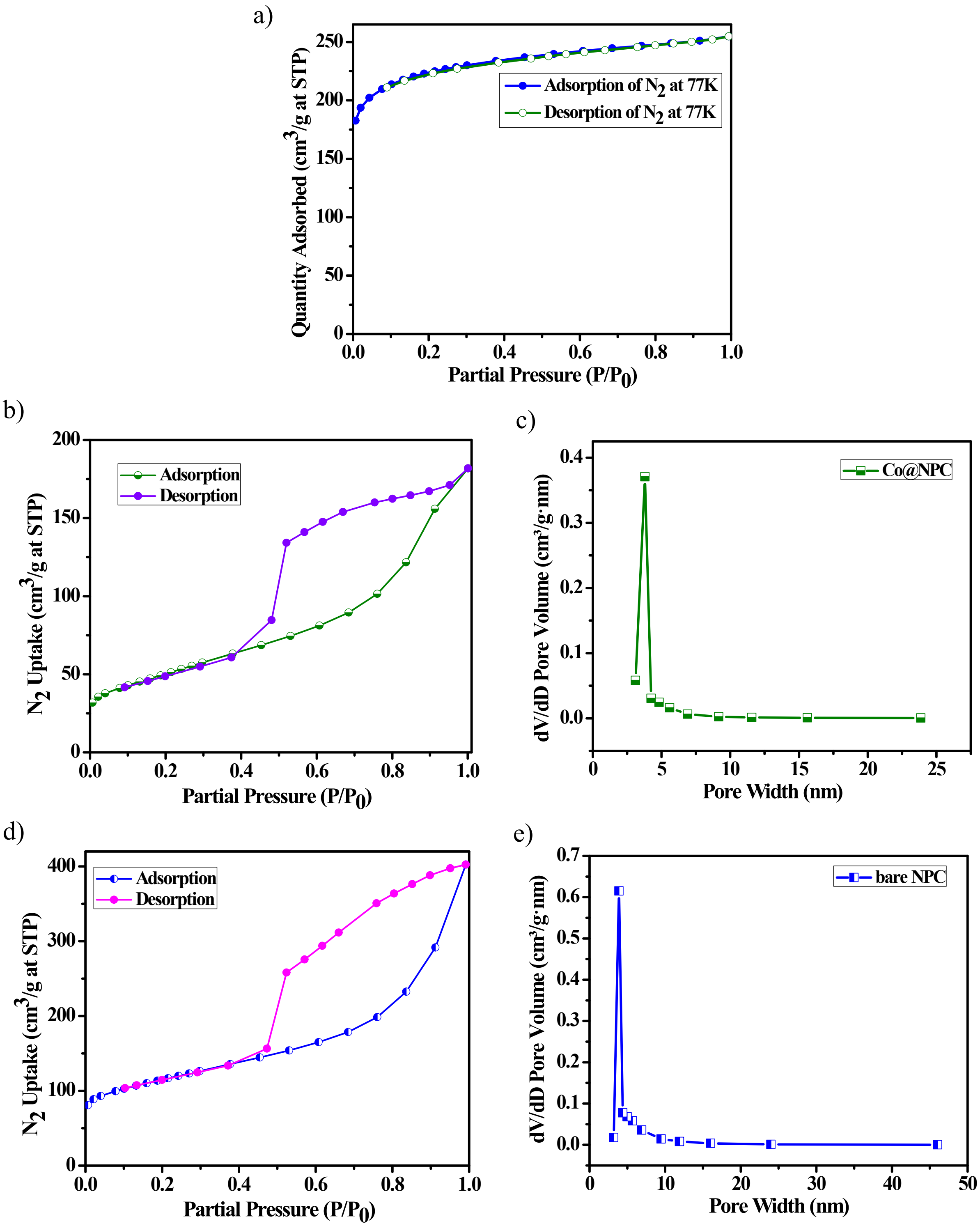

Figure S11. a), b) and d) N_2-adsorption-desorption isotherm of **Co-AOIA**, **Co@NPC** and bare **NPC**, respectively, at 77K and 1 bar pressure; c) and e) pore-size distribution plot for **Co@NPC** and bare **NPC** respectively.

Section S10: X-ray Photoelectron Spectroscopic (XPS) Analysis

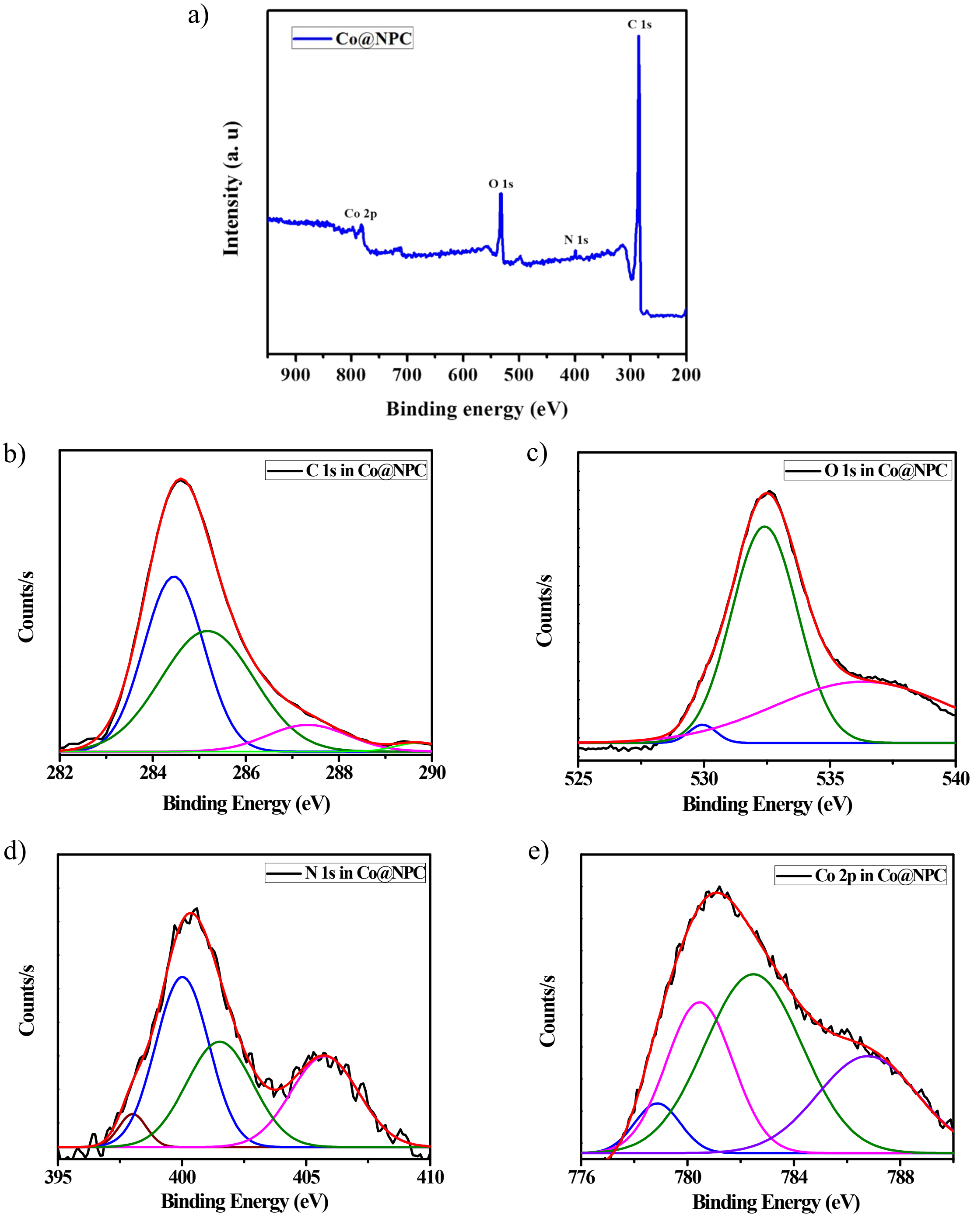

Figure S12. a) XPS full survey spectra of **Co@NPC**; b) High-resolution XPS C 1s spectrum of **Co@NPC**; c) High-resolution XPS O 1s spectrum of **Co@NPC**; d) High-resolution XPS N 1s spectrum of **Co@NPC**; e) High-resolution XPS Co 2p spectrum of **Co@NPC**.

Section S11: Electrochemical Measurements

The electrochemical measurements were carried out in a standard three-electrode system on an electrochemical work station with a CHI 760D (CH Instruments, Inc., USA), in an electrolyte solution of 1 M NaOH. The Platinum (Pt) wire was used as the counter electrode and the saturated calomel electrode (SCE) as the reference electrode. The working electrode was sample coated rotating disk glassy carbon electrode (GCE). For the fabrication of the working electrode, 2 mg of the as-synthesized catalyst (**Co@NPC**) was dispersed in a mixture of distilled water and ethanol (3:1 v/v, 1 ml). 10 µl of Nafion (5 wt%) was added to this solution. The resulting solution was sonicated for at least 40 minutes to prepare a homogeneous ink. 7 µl of this solution was then drop-casted onto the glassy carbon electrode (geometrical surface area: 0.07 cm^2), used as the working electrode for various electrochemical measurements. All potentials measured in this work were referenced to the reversible hydrogen electrode (RHE), according to the Nernst equation: $E_{RHE} = E_{SCE} + 0.242 + 0.059pH$.

To investigate the electrochemical activity of **Co@NPC** towards OER and HER in 1 M NaOH solution, linear sweep voltammetry (LSV) was carried out at 5 mV/s for the polarization curves and Tafel plots. Cyclic Voltammetry (CV) was conducted in N_2 saturated 1 M NaOH electrolyte at room temperature to test the catalytic property of **Co@NPC**. Further, the catalyst was cycled for at least 30 times by CVs with a scan rate of 100 mV/s for activation before LSV testing. Thereafter, the stability and durability of the catalyst were evaluated by potential cycling at a sweep rate of 100 mV/s for 1000 cycles and chronoamperometric measurements.

The overall water splitting was performed in 1 M NaOH solution, as the electrolyte, using a two-electrode cell with **Co@NPC** coated graphite sheets (1 cm^2) as both anode and cathode. For the fabrication of both the electrodes, 2 mg of the as-synthesized catalyst was dispersed in a mixture of distilled water and ethanol (3:1 v/v, 1 ml) with 10 µl of Nafion (5 wt%) solution and 1 ml NMP. The mixture solution was sonicated for at least half an hour to maintain a proper homogeneity. 50 µl of this catalyst ink was then drop-casted over 1 cm^2 graphite sheet and air dried at room temperature for electrochemical measurements.

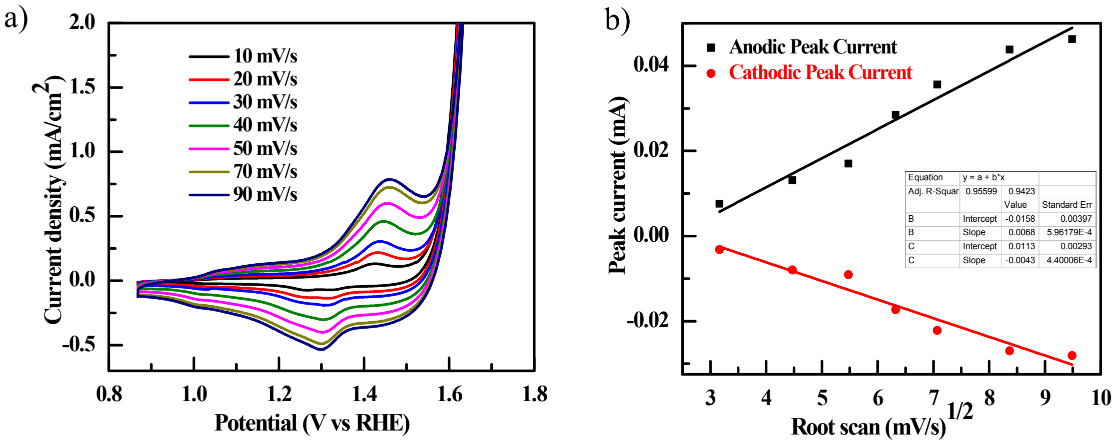

Equation	y = a + b*x		
Adj. R-Squar	0.95599	0.9423	
		Value	Standard Err
B	Intercept	-0.0158	0.00397
B	Slope	0.0068	5.96179E-4
C	Intercept	0.0113	0.00293
C	Slope	-0.0043	4.40006E-4

Figure S13. a) Cyclic voltammogram (CV) of **Co@NPC** at various scan rates in 1 M NaOH solution; b) variation of peak current with scan rate.

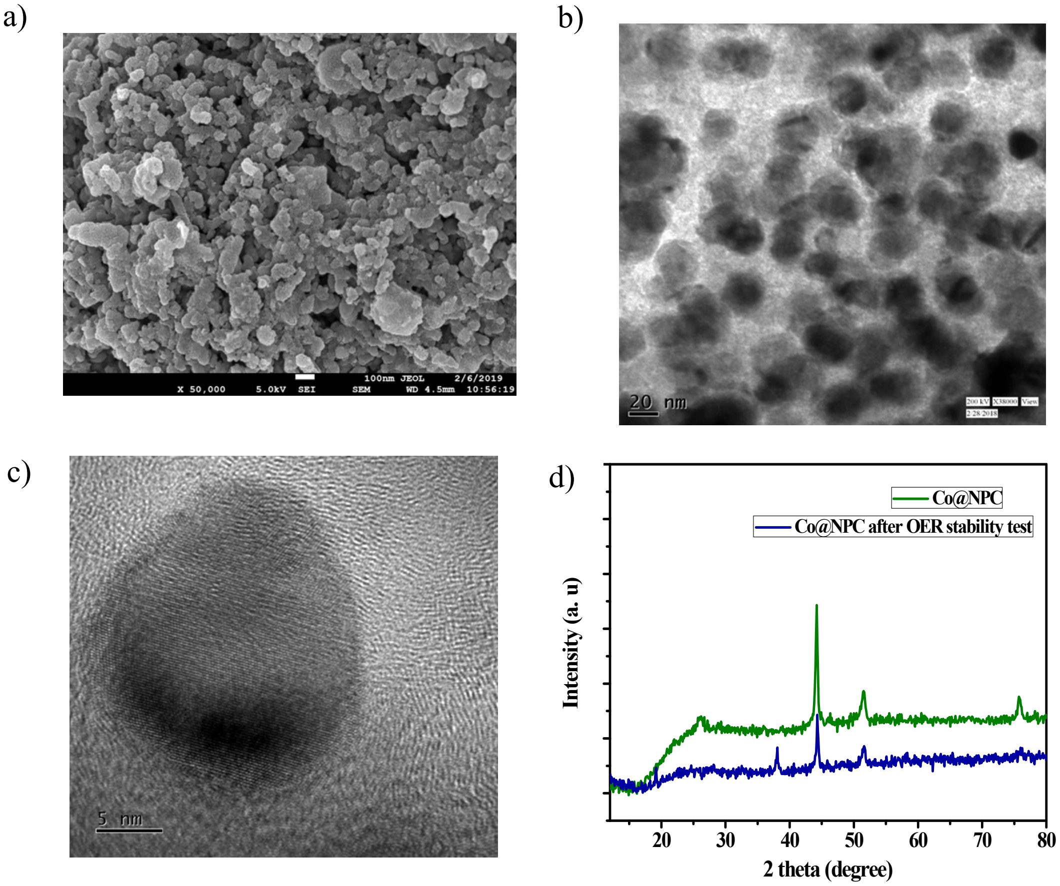

Figure S14. a) FESEM image of **Co@NPC** after OER durability test; b) corresponding TEM image; c) HRTEM image of a single Co nanoparticle of **Co@NPC** after 1000 CV cycles in OER; d) powder patterns of **Co@NPC** after OER stability test.

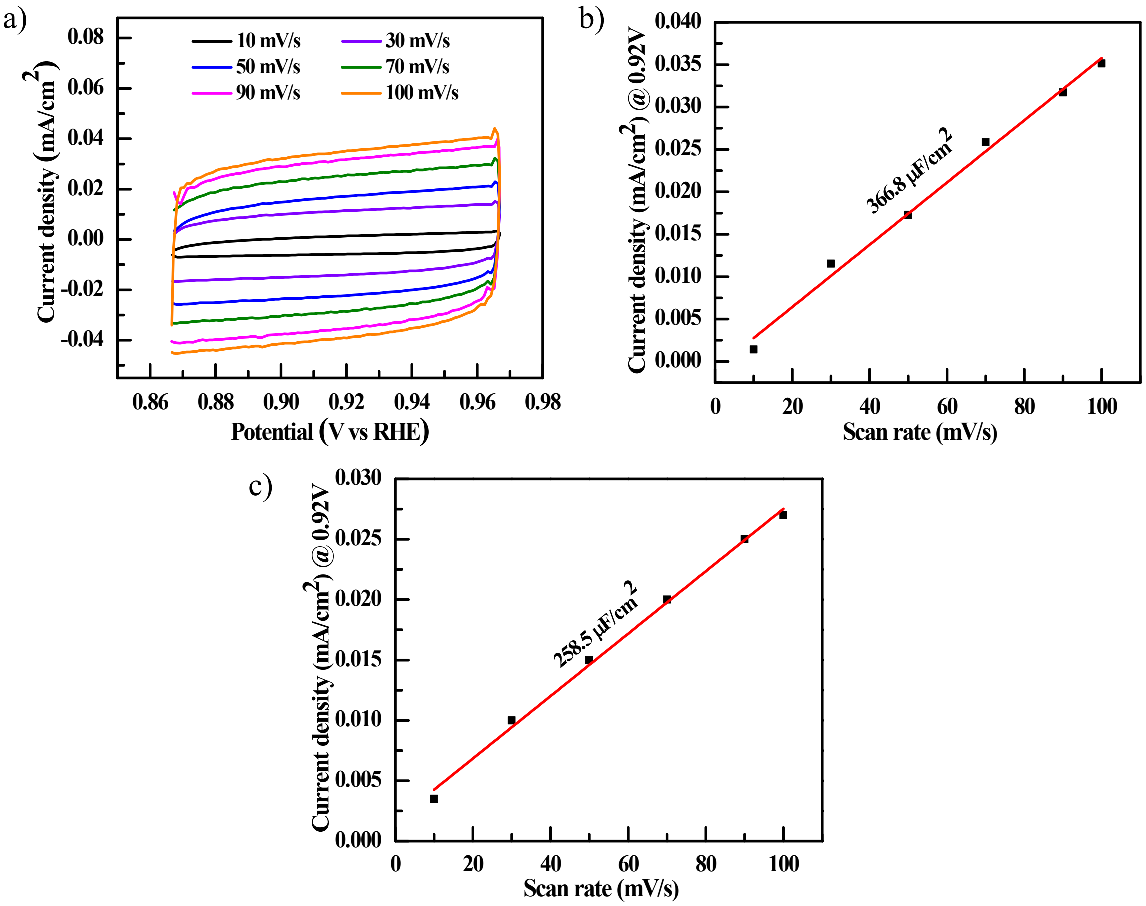

Figure S15. a) CV at various scan rates in the non-Faradaic region for **Co@NPC**; capacitive current density as a function of scan rate in the non-faradaic region, to evaluate C_{dl} for b) **Co@NPC**; c) N-doped porous carbon (bare **NPC**).

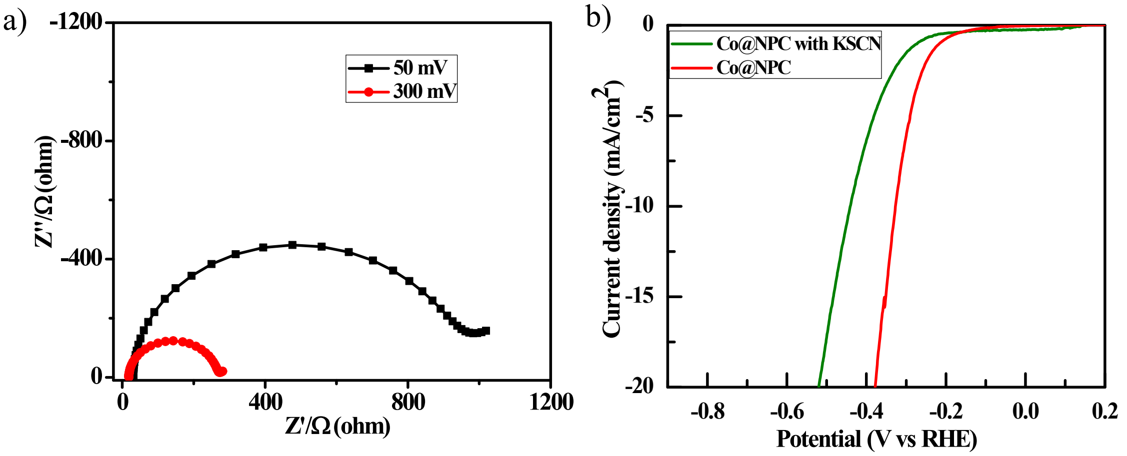

Figure S16. a) Electrochemical impedence spectra (EIS) for Nyquist Plot in **Co@NPC**, at a frequency of 100 KHz to 0.01 Hz; b) HER polarization curve for **Co@NPC** with and without the addition of SCN^- in 1 M NaOH solution.

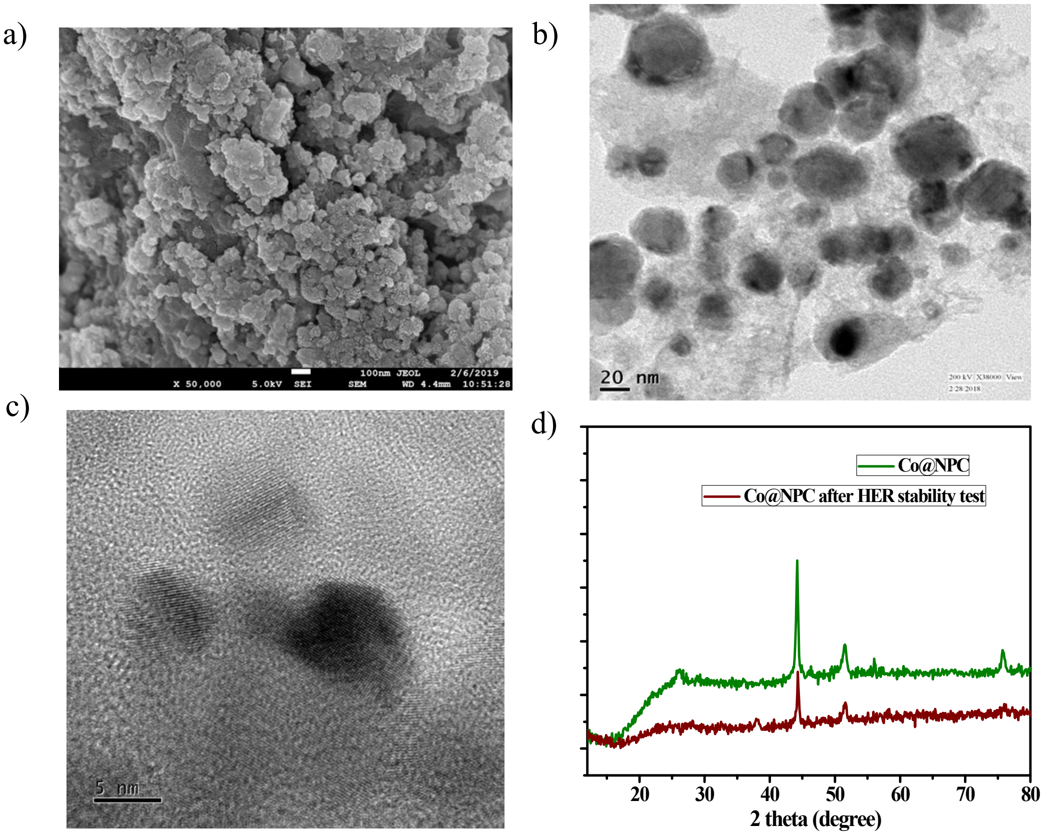

Figure S17. a) FESEM image of **Co@NPC** after HER durability test; b) corresponding TEM image; c) HRTEM image of a single Co nanoparticle of **Co@NPC** after 1000 CV cycles in HER; d) powder patterns of **Co@NPC** after HER stability test.

Section S12: Control Experiments

Synthesis of pristine CoO NPs and Co NPs:

Pure $Co(NO_3)_2$ was dissolved in DMF without the ligand **H_4AOIA** and the mixture solution was heated and then dried. The resulting precipitate was then carbonized at 800^{o}C under argon atmosphere for 4 hrs at a heating rate of 10^{o}C/min, leading to the formation of pristine CoO NPs, as confirmed from the powder XRD patterns (JCPDS file no. 43-1004).

Further, for the preparation of Co NPs, the as-obtained CoO NPs were further annealed at 600^{o}C under a H_2/Ar mixture gas flow for a period of 4 hrs at the same heating rate of 10^{o}C/min.

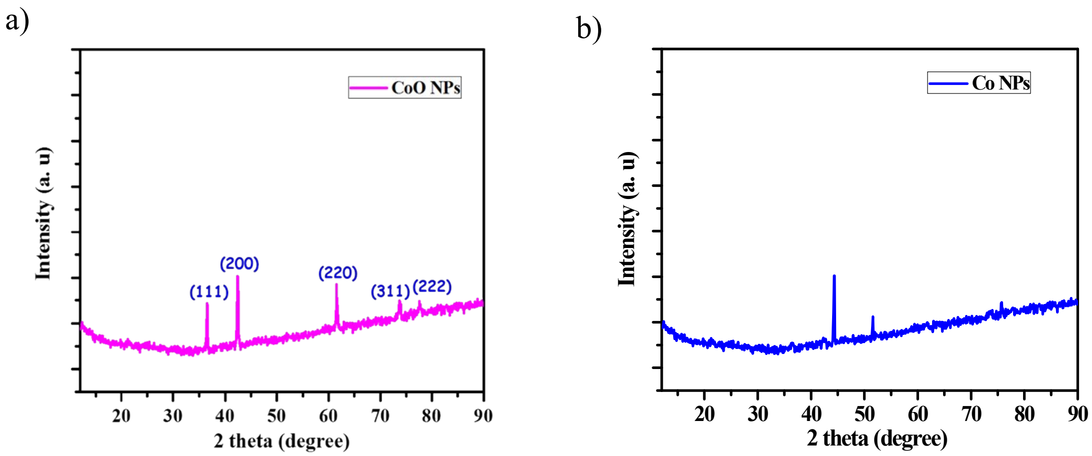

Figure S18. a) Powder patterns of CoO nanoparticles; b) powder patterns of Co nanoparticles.

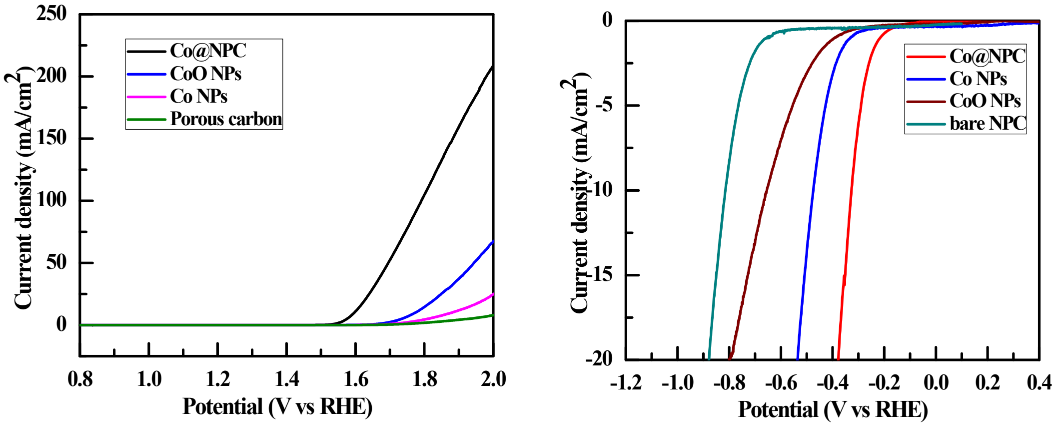

Figure S19. a) OER polarization curves of various catalysts; b) HER polarization curves of various catalysts.

Table S2: Comparison Table of various Co-based electrocatalysts for OER in alkaline media (pH = 14)

Catalysts	Overpotential @j_{10}/mV	Tafel slope (mV/dec)	References
CoP	400	57	S3.
C-Co NPs	390	_	S4.
CoCo LDH	393	59	S5.
CoP/NCNHP	310	70	S6.
Co@Co_3O_4@NC-900	380	94	S7.
Co@NC-3/1	370	90	S8.
PNC/Co	370	76	S9.
Co/HNCP Co_3O_4/HNCP-20 Co_3O_4/HNCP-40 Co_3O_4/HNCP-60 Co_3O_4/HNCP-90	383 369 333 351 358	81 78 69 65 66	S10.
NCNT/CoO-Co	380	64	S11.
Co_2P/Co foil	319	79	S12.
Co@NPC	360	53	**This work**

<u>Table S3</u>: Comparison Table of various Co-based electrocatalysts for HER in alkaline media (pH = 14)

Catalysts	**Overpotential @j_{10}/mV**	**Tafel slope (mV/dec)**	**References**
Co-NRCNTs	370	-	S13.
Co-S/FTO	480	-	S14.
PNC/Co	298	131	S9
N-Co@G	337	-	S15.
Co@NG	220	112	S16.
Co-NC	284	158	S17.
Co-P/Co-PO_4	280	-	S18.
Co@NPC	325	117	**This work**

Table S4: Comparison Table of various Co-based electrocatalysts for overall water splitting in alkaline media (pH = 14)

Catalysts	Electrolyte	Cell Voltage @ j_{10} / V	References
Co_3O_4 nanocrystals	1 M KOH	1.91	S19.
$NiCo_2S_4$	1 M KOH	1.68	S20.
CoP/rGO	1 M KOH	1.7	S21.
Co-S sheets	1 M KOH	1.743	S22.
$Co_{0.85}Se$/NiFe-LDH	1 M KOH	1.67	S23.
Co_2B	1 M KOH	1.81	S24.
CoP/NCNHP	1 M KOH	1.64	S6.
CoP NS/CC	1 M KOH	1.67	S25.
Co@NPC	1 M NaOH	1.66	**This work**

References:

S1. L. P. Zhou and Q.-F. Sun, *Chem. Commun.*, 2015, **51**, 16767–16770.

S2. Sheldrick, G. M. *SHELXL-2014*; University of Göttingen and Bruker AXS: Karlsruhe, Germany, 2014.

S3. M. Liu and J. Li, *ACS Appl. Mater. Interfaces*, 2016, **8**, 2158–2165.

S4. L. Wu, Q. Li, C. H. Wu, H. Zhu, A. Mendoza-Garcia, B. Shen, J. Guo and S. Sun, *J. Am. Chem. Soc.*, 2015, **137**, 7071–7074.

S5. F. Song and X. Hu, *Nat. Commun.*, 2014, **5**, 4477.

S6. Y. Pan, K. Sun, S. Liu, X. Cao, K. Wu, W. C. Cheong, Z. Chen, Y. Wang, Y. Li, Y. Liu, D. Wang, Q. Peng, C. Chen and Y. Li, *J. Am. Chem. Soc.*, 2018, **140**, 2610–2618.

S7. Z. Guo, F. Wang, Y. Xia, J. Li, A. G. Tamirat, Y. Liu, L. Wang, Y. Wang and Y. Xia, *J. Mater. Chem. A*, 2018, **6**, 1443–1453.

S8. Y. Li, B. Jia, Y. Fan, K. Zhu, G. Li and C. Y. Su, *Adv. Energy Mater.*, 2017, **8**(9), 1702048.

S9. X. Li, Z. Niu, J. Jiang and L. Ai, *J. Mater. Chem. A*, 2016, **4**, 3204–3209.

S10. D. Ding, K. Shen, X. Chen, H. Chen, J. Chen, T. Fan, R. Wu and Y. Li, *ACS Catal.*, 2018, **8**, 7879–7888.

S11. X. Liu, M. Park, M. G. Kim, S. Gupta, G. Wu and J. Cho, *Angew. Chem., Int. Ed.*, 2015, **54**, 9654–9658.

S12. C.-Z. Yuan, S.-L. Zhong, Y.-F. Jiang, Z. K. Yang, Z.-W. Zhao, S.-J. Zhao, N. Jiang and A.-W. Xu, *J. Mater. Chem. A*, 2017, **5**, 10561–10566.

S13. X. Zou, X. Huang, A. Goswami, R. Silva, B. R. Sathe, E. Mikmerova and T. Asefa, *Angew. Chem., Int. Ed.*, 2014, **53**, 4372–4376.

S14. Y. Sun, C. Liu, D. Grauer, J. Yano, J. Long, P. Yang and C. Chang, *J. Am. Chem. Soc.*, 2013, **135**, 17699–17702.

S15. H. L. Fei, Y. Yang, Z. W. Peng, G. D. Ruan, Q. F. Zhong, L. Li, E. L. G. Samuel and J. M. Tour, *ACS Appl. Mater. Interfaces*, 2015, **7**, 8083–8087.

S16. M. Zeng, Y. L. Liu, F. P. Zhao, K. Q. Nie, N. Han, X. X. Wang, W. J. Huang, X. N. Song, J. Zhong and Y. G. Li, *Adv. Funct. Mater.,* 2016, **26**, 4397–4404.

S17. F. Yang, P. Zhao, X. Hua, W. Luo, G. Cheng, W. Xing and S. Chen, *J. Mater. Chem. A*, 2016, **4**, 16057–16063.

S18. Y. Yang, H. Fei, G. Ruan and J. M. Tour, *Adv. Mater.*, 2015, **27**, 3175–3180.

S19. S. Du, Z. Ren, J. Zhang, J. Wu, W. Xi, J. Zhu and H. Fu, *Chem. Commun.*, 2015, **51**, 8066–8069.

S20. D. Liu, Q. Lu, Y. Luo, X. Sun and A. M. Asiri, *Nanoscale*, 2015, **7**, 15122–15126.

S21. L. Jiao, Y. Zhou and H. Jiang, *Chem. Sci.*, 2016, **7**, 1690–1695.

S22. J. Wang, H.-X. Zhong, Z.-L. Wang, F.-L. Meng and X.-B. Zhang, *ACS Nano*, 2016, **10**, 2342–2348.

S23. Y. Hou, M. R. Lohe, J. Zhang, S. Liu, X. Zhuang and X. Feng, *Energy Environ. Sci.*, 2016, **9**, 478–483.

S24. J. Masa, P. Weide, D. Peeters, I. Sinev, W. Xia, Z. Sun, C. Somsen, M. Muhler and W. Schuhmann, *Adv. Energy Mater.*, 2016, **6**, 1502313.

S25. W. Zhu, W. Zhang, Y. Li, Z. Yue, M. Ren, Y. Zhang, N. M. Saleh and J. Wang, *J. Mater. Chem. A*, 2018, **6**, 24277–24284.